Sinusoidal phase-modulating laser diode interferometer for real-time surface profile measurement

Guotian He (何国田)[1,3], Xiangzhao Wang (王向朝)[1], Aijun Zeng (曾爱军)[2], and Feng Tang (唐 锋)[1]

[1]*Shanghai Institute of Optics and Fine Mechanics, Chinese Academy of Sciences, Shanghai 201800*

[2]*Shanghai Hengyi Optics & Fine Mechanics Co., Ltd., Shanghai 201800*

[3]*Graduate School of the Chinese Academy of Sciences, Beijing 100039*

Received October 25, 2006

A sinusoidal phase-modulating (SPM) laser diode (LD) interferometer for real-time surface profile measurement is proposed and its principle is analyzed. The phase signal of the surface profile is detected from the sinusoidal phase-modulating interference signal using a real-time phase detection circuit. For 60×60 measurement points of the surface profile, the measuring time is 10 ms. A root mean square (RMS) measurement repeatability of 3.93 nm is realized, and the measurement resolution reaches 0.19 nm.

OCIS codes: 120.3180, 220.4840, 230.5750.

Many kinds of sinusoidal phase-modulating (SPM) laser diode (LD) interferometers have been proposed in the past years[1−5]. In the SPM interferometers, LD is used as the light source. Because the wavelength of the LD can be controlled by its injection current, the phase modulation required by the interferometer is easily produced by modulating the injection current of the LD. The SPM LD interferometers have many merits such as compactness, light weight, easy modulation, and high efficiency[6−8]. The interferometers can be used to measure the surface profile, displacement, vibration, and angle etc.[9−15].

With the development of precise manufacturing, real-time and precision surface profile measurement becomes more and more important. There are mainly three types of SPM LD interferometers used for the surface profile measurement. One is Fourier transform method[3], which is a non-real-time surface profile measurement technique. The other two are phase-lock method[5] and integrating-bucket method[11], which are both real-time measurement techniques. For the phase-lock method, when the amplitude of the interference signal fluctuates due to the external disturbances, a reset control of the peak-hold circuit is required. However, it is difficult to reset this control exactly. The integrating-bucket method can obtain a serial data acquisition rate of 10 μs/point and a measurement repeatability of $\sim \lambda/60$, but the discrimination condition, i.e. the efficiency of $\sin\alpha(x,y)$ equals that of $\cos\alpha(x,y)$, the sinusoidal phase modulation depth $z = 2.45$, and the initial phase of the sinusoidal phase modulation $\theta = 56^{\circ}$[11], is difficult to meet in practice. Furthermore, the phase-lock method and the integrating-bucket method require complex electronic circuits for feedback control, the time delay of the signal processing is relatively long.

In this paper, we propose a novel real-time surface profile measurement system. In this system, the phase signal can be obtained directly from the interference signal using a real-time phase detection circuit. The integrating-bucket discrimination condition is not required. The measurement accuracy is improved and the measurement time is reduced with simple processing circuits.

The SPM LD interferometer for real-time surface profile measurement is shown in Fig. 1. A LD is used as the light source. After collimated and expanded by a lens L1, the beam from the LD is split into two beams by a beam splitter (BS). One beam is reflected by a mirror (M) and used as the reference beam, the other is reflected by the object to be measured and used as the object beam. The interference is formed by the two beams. The interference signal is detected by a charge-coupled device (CCD) image sensor, and is input to a real-time phase detection circuit. The real-time phase detection circuit is shown in Fig. 2. It consists of two amplifiers, a calculator, a low-pass filter (LPF), and a sequential control circuit. After amplified, calculated, and filtered, the interference signal is transformed into phase signal. With the real-time discrimination circuit,

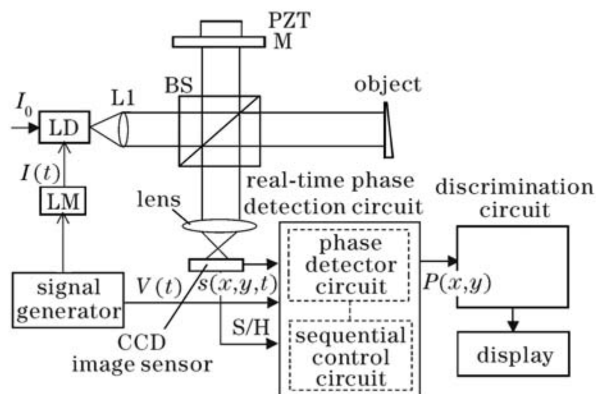

Fig. 1. Diagram of the SPM LD interferometer for real-time surface profile measurement. S/H: sample/hold signal.

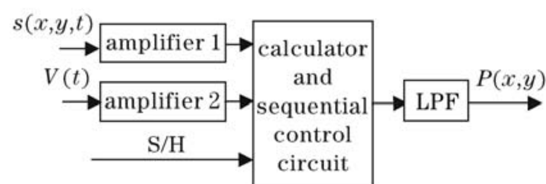

Fig. 2. Block diagram of the real-time phase detection circuit.

1671-7694/2007/030164-04 © 2007 Chinese Optics Letters

the surface profile can be obtained in real time.

The modulation voltage signal of the LD is generated by a signal generator. The sinusoidal modulation signal can be given by

$$V(t) = A\cos\omega_c t, \quad (1)$$

where A is the amplitude of the modulation voltage signal, ω_c is the angular frequency of the sinusoidal modulation signal. The signal $V(t)$ is transformed into a sinusoidal modulation current $I_m(t)$ by a LD modulator LM, and

$$I_m(t) = a\cos\omega_c t, \quad (2)$$

where $a = K_{LM}A$, K_{LM} is the conversion coefficient of the LM. The injection current of the LD consists of the modulation current $I_m(t)$ and a direct current (DC) I_0. The wavelength change of the LD is $\beta I_m(t)$, β is the wavelength modulation coefficient. The interference signal detected by the CCD is given by[15]

$$s(x,y,t) = s_0 + s_1\cos[z\cos\omega_c t + \alpha(x,y)], \quad (3)$$

where s_0 is the DC component of the interference signal, s_1 is the amplitude of the alternating current (AC) component, and z is the sinusoidal phase modulation depth and $z = 4\pi K_{LM}A\beta D_0/\lambda_0^2$, $2D_0$ is the initial optical path difference (OPD) between the two arms of interferometer and λ_0 is the central wavelength of the LD which is determined by the DC I_0. The phase $\alpha(x,y)$ is given by

$$\alpha(x,y) = \alpha_0 + \alpha_r(x,y), \quad (4)$$

where α_0 is the initial phase determined by the optical path difference $2D_0$, $\alpha_0 = K_d D_0$; $\alpha_r(x,y)$ is the phase determined by the surface profile $r(x,y)$, $\alpha_r(x,y) = K_d r(x,y)$; $K_d = 4\pi/\lambda_0$.

Expanding Eq. (3) and neglecting the DC component, we have[11]

$$s(x,y,t) = s_1\{\cos\alpha(x,y)[J_0(z) - 2J_2(z)\cos 2\omega_c t + \cdots]$$
$$-\sin\alpha(x,y)[2J_1(z)\cos\omega_c t - 2J_3(z)\cos 3\omega_c t + \cdots]\}, \quad (5)$$

where $J_n(z)$ is the nth order Bessel function. The interference signal $s(x,y,t)$ detected by the CCD and the modulation signal are amplified by the amplifiers 1 and 2, respectively. Under the control of the sequential circuit, multiplying $s(x,y,t)$ by $V(t)$ in the same time and passing it through the LPF, we obtain the phase signal $P(x,y)$. The gain of the amplifier1 is K_1, that of amplifier 2 is K_2; the coefficient of the calculator is K_3; the gain of the LPF is K_4. The cut-off frequency is less than $\omega_c/8$. Therefore, the phase signal $P(x,y)$ is given by

$$P(x,y) = K_1K_2K_3K_4s_1AJ_1(z)\sin\alpha(x,y). \quad (6)$$

We define

$$K_p = K_1K_2K_3K_4s_1AJ_1(z). \quad (7)$$

Then

$$\alpha(x,y) = \arcsin[P(x,y)/K_p]. \quad (8)$$

Neglecting the DC component α_0 in $\alpha(x,y)$, the surface profile can be expressed as

$$r(x,y) = \arcsin[P(x,y)/K_p]/K_d. \quad (9)$$

If the constant K_p is known and the phase signal $P(x,y)$ is obtained in real time from the signal $s(x,y,t)$, the object surface profile will be measured in real time.

The phase $\alpha(x,y)$ can be obtained in real time from the phase signal $P(x,y)$ using a real-time discrimination circuit shown in Fig. 3. The circuit mainly consists of a 10-bit analog/digital (A/D) convertor, a 10-bit read-only memory (ROM), a random access memory (RAM), a digital/analog (D/A) convertor, and a display unit.

The phase values are stored in the ROM and the sinusoidal function values are used as addresses corresponding to the phases to form a look-up table. Table 1 shows the content of the ROM, where addresses 0 and 1023 correspond to $-\pi/2$ and $+\pi/2$, respectively. The resolution of the phase measurement is $\pi/1024$. Each phase value needs 2-byte storage space and the phases need 2k-byte ROM storage spaces. For the CCD image sensor with 100×100 effective pixels, 20-MB ROM is needed. Under the control of the sequential circuit, the A/D convertor can transform the phase signal $P(x,y)$ into a digital signal. The digitalized phase signal $P(x,y)$ serves as the address of the ROM, and the data stored in the ROM address give the phase $\alpha(x,y)$. The phase in the ROM is transferred to the RAM to calculate the surface profile $r(x,y)$ according to Eq. (9). With the D/A convertor, the analog signal of the surface profile can be obtained and displayed in the display unit. Therefore, the surface profile can be obtained in real time.

K_p is related to the modulation depth z and D_0. Because D_0 cannot be measured accurately, K_p cannot be obtained accurately according to Eq. (7). In order to measure K_p accurately, the interferometer is calibrated according with a sinusoidally vibrating mirror attached to a piezoelectric transducer (PZT). The beam reflected from a point (x_0,y_0) of the object surface is used as the reference wave, and the beam reflected from the mirror M is used as the object wave. The interference signal $s(x_0,y_0,t)$ is formed by the two beams[16]. Making

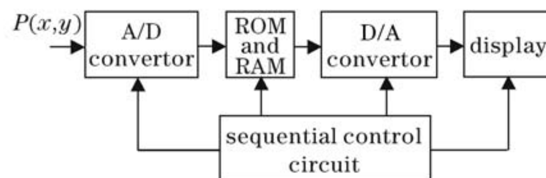

Fig. 3. Block diagram of the real-time discrimination circuit.

Table 1. ROM Addresses and the Corresponding Phase Values

ROM Address	$P(x,y)$	$\alpha(x,y)$
0	$-K_p$	$-\pi/2$
...	...	...
511	0	0
...	...	...
1023	K_p	$\pi/2$

$\alpha(x_0, y_0, t)$ near to $2n\pi$ ($n = 0, 1, 2, \cdots$) by adjusting $\beta(x_0, y_0)$, we can obtain

$$\alpha(x_0, y_0, t) \approx [\beta(x_0, y_0) + P(x_0, y_0, t)]/K_\mathrm{p}, \quad (10)$$

where $\beta(x_0, y_0)$ is the DC component of the phase signal in a point (x_0, y_0) of the object surface. Therefore we can obtain

$$K_\mathrm{p} \approx [\beta(x_0, y_0) + P(x_0, y_0, t)]/[r(x_0, y_0, t)K_\mathrm{d}]. \quad (11)$$

Because K_p is only related to the optical system and the signal processing circuit in the paper, K_p is the same for the displacement measurement and surface profile measurement.

The relation between the vibration amplitude of the PZT and the amplitude of the driving voltage has been calibrated using the method proposed in Ref. [16]. With the voltage loaded to the PZT, we obtained the measured signal $P(x_0, y_0, t)$ of the point (x_0, y_0), and K_p can be obtained using Eq. (11). So, we can obtain the phase signal of the object surface profile using the real-time phase detection circuit.

The experiment was performed using the setup shown in Fig. 1. The LD was with the central wavelength of 785 nm, the output power of 50 mW, and the wavelength modulation coefficient β of 1.56×10^{-2} nm/mA. The gain K_1 of amplifier 1 was 70.2, and K_2 of amplifier 2 was 91.5. The conversion coefficient K_LM of LM was 0.002 mA/mV and the coefficient K_3 of the calculation unit was 5×10^{-5} mV^{-1}. In the experiment, we chose the third order Butterworth LPF with the cut-off frequency of 50 Hz, the gain K_4 was 10. The OPD $2D_0$ was about 6 cm, and the sinusoidal modulation frequency was 200 Hz. The conversion coefficient K_d from surface profile $r(x, y)$ to phase $\alpha(x, y)$ was 1.6×10^{-2} rad/nm. The CCD image sensor had 60×60 effective pixels, and the frame rate was 1600 frame/s. The sampling frequency of the A/D convertor was 8 MHz. The measured object was an optical wedge.

In order to calibrate K_p accurately, the PZT was driven with a sinusoidal signal at the frequency of 50 Hz. So, the PZT was vibrated sinusoidally along the optical axis. The relationship between the driving voltage and the vibration amplitude of the PZT had been calibrated. Using the signal detected by one pixel of the CCD array, K_p was calculated to be 2.28×10^3 mV/rad.

The data of the look-up table were stored in a ROM. First, to check our system, we measured the surface profile of the optical wedge in real time, and the measurement result is shown in Fig. 4(a). Next, using the discrete Fourier transformation (DFT) method[3], the surface profile was measured with the optical path unchanged, the result is shown in Fig. 4(b). The correlation coefficient of the two figures is 0.986, which means that the two measurement results are coincident.

The effective pixels and the frame rate of the CCD image sensor were adjusted to 40×40 and 800 frame/s, respectively. The sinusoidal phase modulation frequency was adjusted to 100 Hz. The surface profile of the optical wedge was measured under this condition, and the result is shown in Fig. 5(a). After ten minutes, the optical wedge was measured again, the result is shown in Fig. 5(b). Figures 5(a) and (b) agree well with each other, the root mean square (RMS) deviation between them is 3.93 nm.

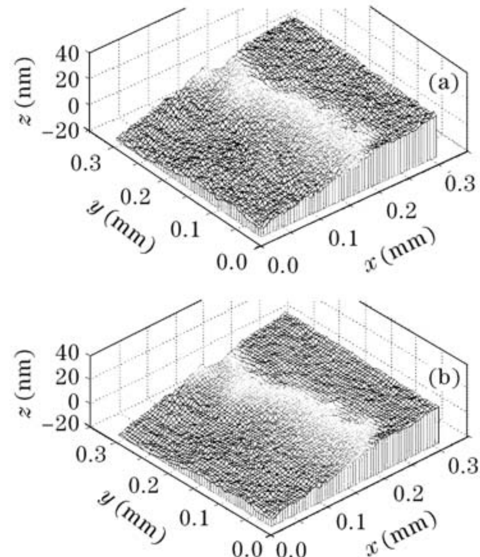

Fig. 4. (a) Real-time and (b) DFT measurement results of the surface profile of an optical wedge.

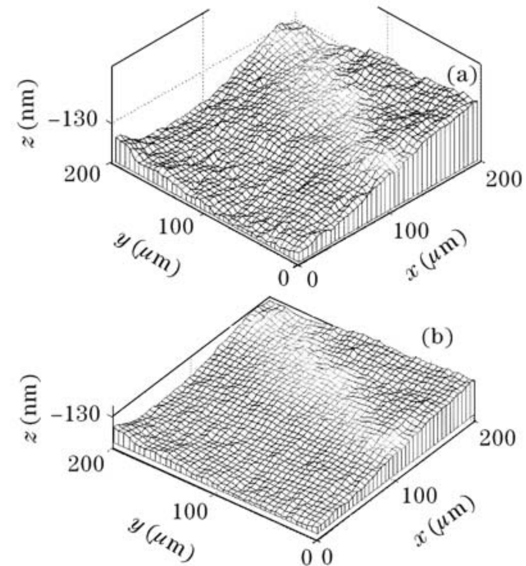

Fig. 5. Repeated measurement results of the surface profile of a gilt mirror show excellent repeatability of the SPM LD interferometer.

In order to analyze the measurement accuracy, the 20th rows of Figs. 5(a) and (b) in the x-direction are shown Fig. 6. The RMS deviation between the two results is 3.78 nm. In the same way, we analyze the 10th column in Fig. 5 and the RMS deviation is 3.71 nm.

The modulation frequency $\omega_\mathrm{c}/2\pi$ of the LD was 100 Hz. The frequency of the phase detection was 1600 frame/s for 16 points in a period. The charge storage period of the CCD was 0.167 ms, and the read time of one field was 0.0835 ms, which was a half of the charge storage period. The readout frequency of each pixel was 8 MHz. Consequently, the measurement time was 10 ms. The number of effective pixels in one frame was 60×60 and the serial data acquisition rate was 2.8 μs/point.

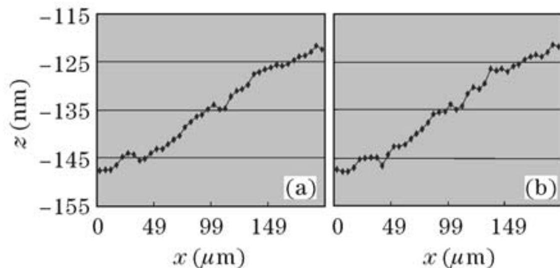

Fig. 6. Surface profiles along x-axis taken from Fig. 5.

The measurement resolution of the system was determined by the digital capacity of the look-up table. In our experiments, a 1024 elements look-up table was adopted, the measurement resolution was 0.192 nm and the maximum measurement range was $\lambda/2$.

In this paper, we have proposed a SPM LD interferometer for real-time surface profile measurement. In this interferometer, the phase signal was obtained directly from the interference signal using a real-time phase detection circuit. In experiments, the repeatability of the measurement was less than 3.93 nm. The measurement time was less than 10 ms. The measurement resolution of the surface profile $r(x,y)$ was 0.19 nm. The measurement range was less than $\lambda/2$.

If the operational frequency could be higher, e.g. 400 Hz, the measurement time would be reduced to 5.0 ms. The measurement time will be shortened further if we use specific high-speed integrated circuits instead of the general digital integrated circuits in the experimental setup.

This work was supported by National Natural Science Foundation of China (No. 60578051) and International Cooperation Program of Shanghai Municipal Science & Technology Commission (No. 051107085). G. He's e-mail address is slhgt@siom.ac.cn.

References

1. H. Akiyama, O. Sasaki, and T. Suzuki, Opt. Express. **13,** 10066 (2005).
2. D. Li, X. Wang, X. Wang, L. Guo, and Y. Liu, Chin. J. Lasers (in Chinese) **31,** 350 (2004).
3. O. Sasaki and H. Okazaki, Appl. Opt. **25,** 3137 (1986).
4. J. Li, O. Sasaki, and T. Suzuki, Opt. Commun. **260,** 398 (2006).
5. T. Suzuki, O. Sasaki, and T. Maruyama, Appl. Opt. **28,** 4407 (1989).
6. O. Sasaki, H. Sasazaki, and T. Suzuki, Appl. Opt. **30,** 4040 (1991).
7. X. Wang, X. Wang, H. Lu, F. Qian, and Y. Bu, Opt. Laser Technol. **33,** 219 (2001).
8. T. Suzuki, S. Hirabayashi, O. Sasaki, and T. Maruyama, Opt. Eng. **38,** 543 (1999).
9. X. Wang, X. Wang, D. Yu, F. Qian, and H. Lu, Acta Opt. Sin. (in Chinese) **21,** 1368 (2001).
10. S. Song, X. Wang, X. Wang, F. Qian, and G. Chen, Chin. J. Lasers (in Chinese) **28,** 753 (2001).
11. T. Suzuki, O. Sasaki, J. Kaneda, and T. Maruyama, Opt. Eng. **33,** 2754 (1994).
12. X. Wang, O. Sasaki, T. Suzuki, and T. Maruyama, Appl. Opt. **39,** 4593 (2000).
13. X. Wang, O. Sasaki, T. Suzuki, and T. Maruyama, Opt. Eng. **38,** 1553 (1999).
14. Y. Liu and X. Wang, Chin. J. Lasers (in Chinese) **33,** 1574 (2006).
15. Y. Liu, X. Wang, and X. Wang, Chin. Opt. Lett. **4,** 309 (2006).
16. X. Wang, X. Wang, F. Qian, G. Chen, G. Chen, and Z. Fang, Opt. Laser Technol. **31,** 559 (1999).